

UNIVERSITY OF SCIENCE AND TECHNOLOGY OF HANOI



THE INTERNATIONAL CENTRE FOR INTERDISCIPLINARY  
SCIENCE AND EDUCATION (ICISE)

---

---

Internship Report

**Study And Observing The  
Performance of Readout Circuit for  
Light Sensitive Photon Sensor**

---

---

<u>Students:</u>	<b>Ton That Minh Bao</b>
<u>Department:</u>	<b>Space and Applications</b>
<u>Academic year:</u>	<b>2021-2022</b>
<u>External Supervisor:</u>	<b>Dr. Cao Van Son</b>
<u>Internal Supervisor:</u>	<b>Dr. Phan Thanh Hien</b>

September 13, 2023

# Contents

<b>1</b>	<b>Introduction</b>	<b>1</b>
1.1	SiPM's structure . . . . .	1
1.1.1	Avalanche photodiode . . . . .	1
1.1.2	Geiger mode . . . . .	2
1.1.3	SiPM's equivalent circuit . . . . .	4
1.2	SiPM's property . . . . .	4
1.2.1	After-pulses . . . . .	4
1.2.2	Optical Crosstalk . . . . .	5
1.2.3	Electrical Gain . . . . .	5
1.2.4	Dark Count rate . . . . .	5
1.2.5	Photon detection efficiency (PDE) . . . . .	6
1.3	Objective . . . . .	7
<b>2</b>	<b>Experiment and Simulation</b>	<b>8</b>
2.1	Experiment . . . . .	8
2.1.1	Introduction . . . . .	8
2.1.2	Instruments . . . . .	8
2.1.3	Experiment Set-up . . . . .	10
2.2	Simulation model . . . . .	11
2.2.1	Assumption . . . . .	11
2.2.2	MPPC and Readout Circuit simulation . . . . .	11
2.2.3	Wave form's characteristic . . . . .	14
2.2.4	Components's parameters . . . . .	15
<b>3</b>	<b>Result and Discussion</b>	<b>19</b>
3.1	Bandwidth Effect to the output waveform . . . . .	19

3.1.1	Simulation result . . . . .	19
3.1.2	Measurement result . . . . .	21
3.2	Effect on waveform due to shaping capacitor . . . . .	22
3.2.1	Simulation result . . . . .	22
3.2.2	Measurement result . . . . .	24
<b>4</b>	<b>Conclusion</b>	<b>26</b>
<b>5</b>	<b>Appendix</b>	<b>I</b>
5.1	Obtain the mean life time of the pulse using exponential fitting . . . . .	I

# List of Figures

1.1	The Avalanche Photodiode's fundamental structure . . . . .	2
1.2	The dependence of gain on the reverse bias . . . . .	3
1.3	APD's geiger mode equivalent circuit, $C_d$ is the capacitance of the avalanche photodiode . . . . .	3
1.4	SiPM's pixel structure . . . . .	4
1.5	After-pulse and Crosstalk pulse when observing signal . . . . .	5
1.6	The dependence of the PDE to incident wavelength and overvoltage at operation temperature [4] . . . . .	6
2.1	Voltage Source and Wave Visualise Instrument . . . . .	9
2.2	MPPC practical readout circuit . . . . .	9
2.3	Multi-pixels photon counter (MPPC) model S13360-1325CS . . . . .	10
2.4	Experimental Setup . . . . .	10
2.5	Readout circuit for MPPC . . . . .	11
2.6	Equivalent circuit for the discharged microcells in MPPC [6] . . . . .	12
2.7	Pulse shape for ideal SiPM [1] . . . . .	14
2.8	Pulse shape in detailed SiPM equivalent circuit [2] . . . . .	14
2.9	Output signal of single P.E waveform simulated by LTspice software when decreasing the value of $C_d$ and increase the value of $C_q$ . . . . .	16
2.10	Output signal of single P.E waveform simulated by LTspice software when decreasing the value of $C_q$ and increase the value of $C_d$ . . . . .	16
2.11	The simulation versus the signal measured at BW of 100 MHz. The simulation result simulated by LTspice software, the measurement data is obtained by SIGLENT SDS 1104X-E 100 MHz Oscilloscope. . . . .	17

2.12	The simulation versus the signal measured at BW of 200 MHz. The simulation result simulated by LTspice software, the measurement data is obtained by SIGLENT SDS 1202X-E 200 MHz Oscilloscope. . . . .	18
3.1	Simulated waveforms of the single P.E event generated by LTspice software at different bandwidth limit, using $C_s = 0.1\mu F$ . . . . .	19
3.2	Simulated waveforms of the single P.E event generated by LTspice software at different bandwidth limit, using $C_s = 1nF$ . . . . .	20
3.3	Data measured with two different Oscilloscope with different BW limit, using shaping capacitor $C_s = 1\mu F$ . Both pulses is averaged with 256 samples. . . . .	21
3.4	Data measured with two different Oscilloscope with different BW limit, using shaping capacitor $C_s = 1nF$ . Both pulses is averaged with 256 samples. . . . .	21
3.5	Simulation results of output waveforms using different capacitors, at BW = 100 MHz. . . . .	22
3.6	Simulation result of output waveforms using different capacitors, at BW = 200 MHz. . . . .	23
3.7	Experimental results of the single P.E output waveforms, measured with different capacitors, the data is obtained using SDS 1104X-E 100MHz Oscilloscope. . . . .	24
3.8	Experimental results of the single P.E output waveforms, measured with different capacitors, the data is obtained using SDS 1202X-E 200MHz Oscilloscope. . . . .	24
5.1	Exponential decay . . . . .	I
5.2	Result of shaping capacitor $C_s = 47pF$ . . . . .	III
5.3	Result of shaping capacitor $C_s = 220pF$ . . . . .	III
5.4	Result of shaping capacitor $C_s = 1nF$ . . . . .	IV
5.5	Result of shaping capacitor $C_s = 10nF$ . . . . .	IV
5.6	Result of shaping capacitor $C_s = 0.1\mu F$ . . . . .	V

# List of Tables

2.1	MPPC S13360-1325CS Data sheet [3] . . . . .	10
5.1	Parameter obtained from the fitting . . . . .	V

# List of Abbreviation

SiPM	Silicon Photomultiplier
MPPC	Multi-pixel photon counter
BW	Bandwidth
APD	Avalanche Photodiode
DC	Direct Current

# Acknowledgements

Firstly, I want to express my gratitude to my supervisor - Dr. Cao Van Son, for allowing me to work on this project. I also want to thank Professor Jean Tran Thanh Van and Dr. Tran Thanh Son for supporting me in working at ICISE.

Secondly, thanks to my family for always being my mental support; I very much appreciate that.

Thirdly, I want to pay my last love to my friends and mentors at ICISE and USTH for always helping me whenever I need it. You guys are very enduring to hear my complaints, friendly, and sometimes strictly give ideas if I make a mistake.

Finally, I am doing an internship with many experiments, so I want to thank the instruments for working well most of the time I use them. Without your contribution, my work will never finish.



# Abstract

SiPM is a very promising device in semiconductor technology due to numerous advantages features such as exceptional high gain, fast response, immunity to magnetic fields, portability, electronical integration, and cost effectiveness. This sensor applies in many aspects: academic research, medicine, transportation, satellite technology,... Studying the characteristic of the SiPM can give the users a better understanding of how this one work and how to apply it to many fields, then people can use this technology efficiently. In this internship, I will study the operation of an actual model of the SiPM from Hamamatsu company by observing the output signal generated by itself when applying the reverse bias. Then I will try to combine the SiPM with the readout circuit to investigate its performance when changing the parts in the circuit. We also reduce noise and try to obtain a better output signal. I also do the simulation using free software to compare the results of the simulation and the experiment to have a good simulation model. This one is constructive for people to work with a more complex model.

# Chapter 1

## Introduction

Silicon Photomultiplier is a solid-state single photon counter that uses multiple **Avalanche photodiode (ADP)** pixels operating in **Geiger mode**. SiPM can provide high electrical gain, good timing resolution, high sensitivity, it can also operate in low voltage, and immunity to the magnetic field.

Due to these advantage, SiPM has a wide range of application:

- Biophotonic: SiPM is widely used in some aspects of Biophotonics, such as Bioimaging Systems, Fluorescence analysis, and spectroscopy.
- High energy physics: Due to the high sensitivity of SiPM, people can make some systems that allow them to detect photons produced when particles pass through a special material called a scintillator. This can also apply to fields like x-ray scanning, isotope identifier,...
- Lidar application: Based on the pulse time-of-flight principle, our system can conduct a hundred-meter measurement using a low-cost system operating in a wide range of temperatures.

### 1.1 SiPM's structure

#### 1.1.1 Avalanche photodiode

- The photodiode is a semiconductor device that transforms photons (optical signal) into current (electrical signal). This mechanism is due to photoelectric effect (which is discovered by Einstein)

- Avalanche photodiode is a type of photodiode that will produce internal gain when applying reverse voltage. Unlike photodiode, which provide a single electron-hole pair for each incoming photon. In avalanche breakdown, the gain  $< 10^3$ .
- Avalanche diode's structure

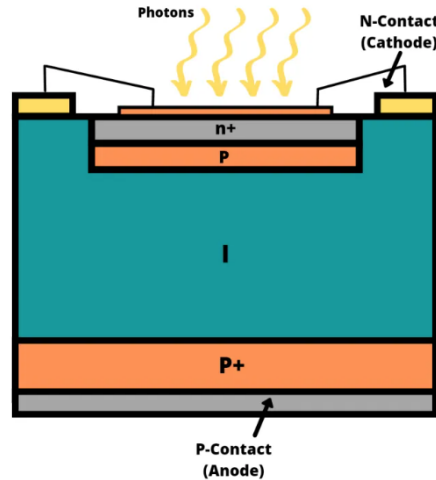


Figure 1.1: The Avalanche Photodiode's fundamental structure

- ADP comprises four central regions, divided into two types:  $n+, p+$  region, heavily doped, and  $I, p$  lightly doped.
- In the ADP, the  $p+$  region acts like an anode, and the  $n+$  region acts like a cathode.

### 1.1.2 Geiger mode

An electric field will generate when applying a reverse bias voltage into the avalanche diode. Electrons start to gain kinetic energy, and they then start to break the covalent bonds and create e-hole pairs; these pairs travel and accelerate, then collide with other atoms, resulting in a large number of e-hole pairs. This is called **geiger mode** and happened at a voltage above the breakdown voltage [1].

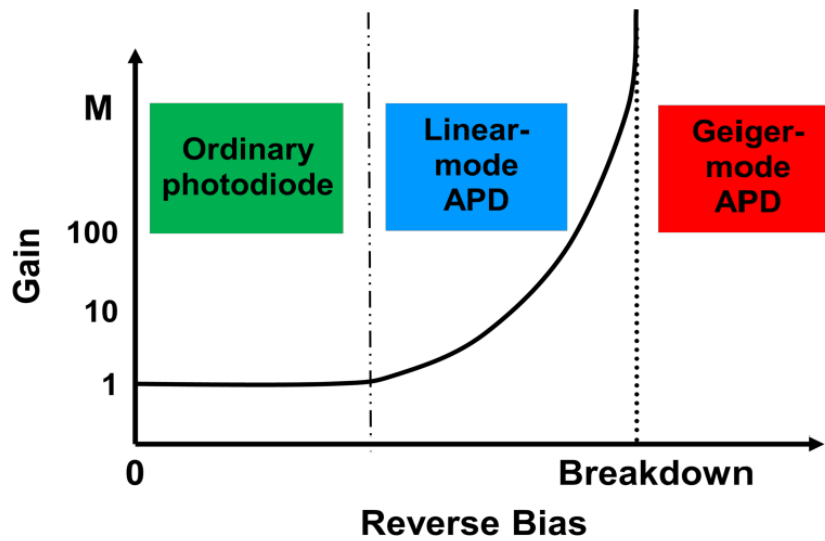


Figure 1.2: The dependence of gain on the reverse bias

1. Equivalent Circuit of a geiger mode avalanche photodiode (APD)

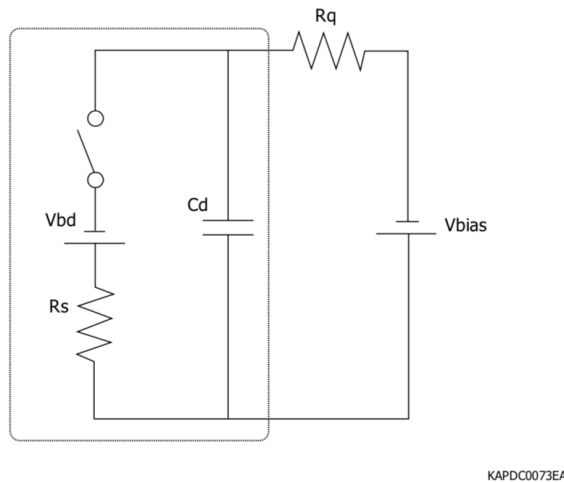


Figure 1.3: APD's geiger mode equivalent circuit,  $C_d$  is the capacitance of the avalanche photodiode

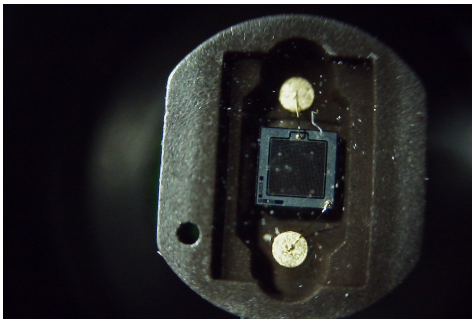
- When a photon(s) comes in and interact with lattice or when there is a thermal effect that generates electron/hole pair, the "switch" close, then capacitor  $C_d$  discharge through  $R_s$ , the voltage increase
- We can determine the net current  $I_d$  using two loops, then have the equation:

$$I_d = (V_d - V_{bd})/R_s + (V_{bias} - V_d)/R_q$$

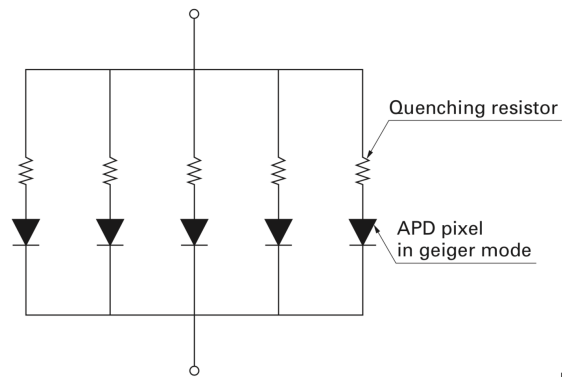
- Since one side of the current flow is to charge, and the other is to discharge the capacitor, these currents are in the opposite direction
- When the discharge process is exhausted, the avalanche process is quenched, and the "switch" open again.
- The recharge current flow through  $R_q$  then increase voltage across  $C_d$  by  $(V_{bias} - V_{bd})$  to equal  $V_{bias}$

### 1.1.3 SiPM's equivalent circuit

Silicon Photomultiplier (SiPM) is a matrix of pixels, where each pixel is composed of an APD and a quenching resistor to be a "small circuit." Those "small circuits" connect in parallel to become a SiPM.



(a) A close look of multipixel SiPM structure



KAPDC0029EA

(b) SiPM's equivalent circuit

Figure 1.4: SiPM's pixel structure

## 1.2 SiPM's property

### 1.2.1 After-pulses

This phenomena often happen during avalanche process. There is a small portion of charge carriers get trapped in the impurity energy level but will release after short delay when receiving energy, then they will re-enter the valence or the conduction band.

## 1.2.2 Optical Crosstalk

When observing the output pulse, we may observe some spurious pulses. After suffering scatter collision, the energy is often lost as heat phonon vibration. However, there is a probability that the energy will be emitted as a photon. This one can travel to the neighbor pixel and trigger the avalanche process.

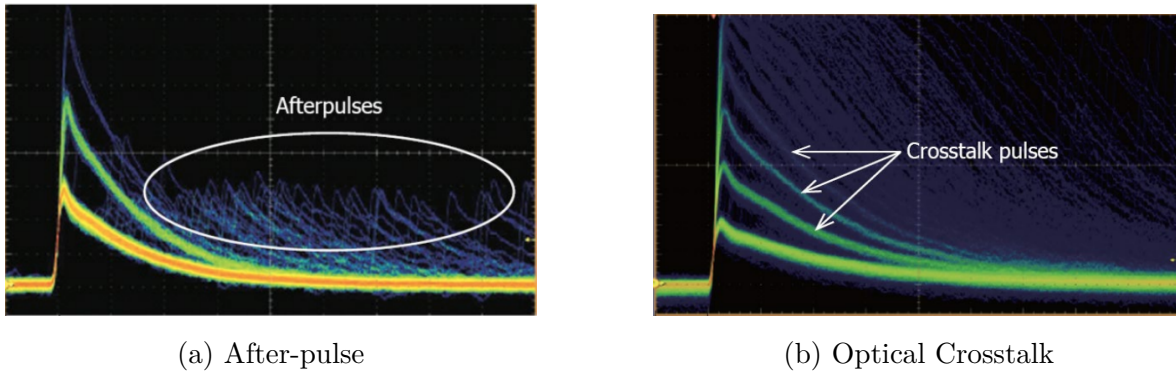


Figure 1.5: After-pulse and Crosstalk pulse when observing signal

## 1.2.3 Electrical Gain

Electrical gain is defined as the total charge of the pulse generated from the SiPM when detect a photon divide to the charge of an electrons. Electrical gain is dependence to the overvoltage and the operational temperature

$$G = \frac{Q}{q} = C \times \frac{V_{bias} - V_{br}}{q}$$

Where  $Q$  is the total charge of the pulse,  $q$  is the charge of electron ( $q = 1.6 \times 10^{-19}C$ ),  $C$  is the capacitance of the SiPM's pixel,  $V_{bias}$  and  $V_{br}$  in turn is the bias voltage and the break down voltage.

## 1.2.4 Dark Count rate

The carrier is generated by the thermal effect inside of the SiPM. The pulse created by these carriers is called a dark pulse. The number of dark pulses observed depends on the temperature and the overvoltage. The number of dark pulses is called "dark count", then the number of dark pulses observed in a second is defined "as dark count rate".

### 1.2.5 Photon detection efficiency (PDE)

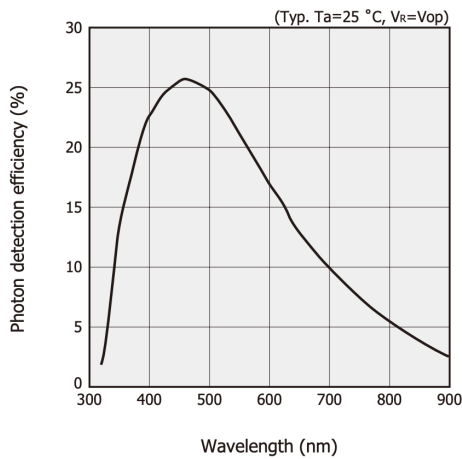
Photon detection efficiency (PDE) is defined as the ratio of the number of detected photons to the number of incident photons. PDE can also express as:

$$PDE = F_g \times QE \times Pa$$

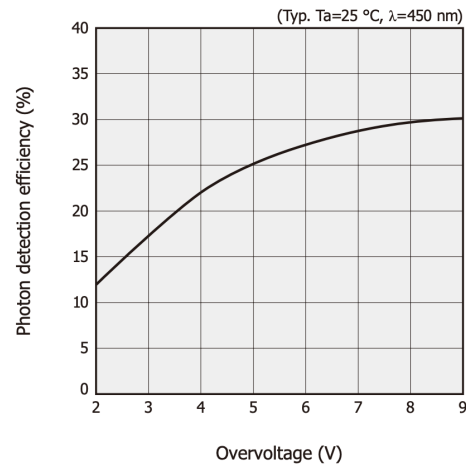
Where

- $F_g$  is the filling factor, which is the ratio between the light detectable area and the pixel's total area.
- QE is the quantum efficiency. QE is defined as the effectiveness of converting an incident photon to the electron-hole pair. This parameter depends on the wavelength of incident light.
- $Pa$  is the avalanche probability, the quantity to describe the probability of causing the avalanche process of the carrier.

PDE depends largely on the overvoltage and the wavelength of the incident light.



(a) PDE vs overvoltage (pixel pitch  $25\mu m$ )



(b) PDE vs overvoltage (pixel pitch  $25\mu m$ )

Figure 1.6: The dependence of the PDE to incident wavelength and overvoltage at operation temperature [4]

## 1.3 Objective

In this internship, we will:

- Exploring and measuring the property of the SiPM device
- Study the readout circuit and try to simulate the circuit using LTspice software
- Study the Bandwidth effect in observing the signal
- Study the effect of shaping capacitor on the output signal



# Chapter 2

## Experiment and Simulation

### 2.1 Experiment

#### 2.1.1 Introduction

In our experiment, instead of using the signal generated by the photoelectric effect, we will conduct the experiment in a "dark state" by covering the SiPM. In this state, the pulse is only constructed by thermally-generated carriers. The SiPM type we will use in the experiment is a product from the Hamamatsu company, this type of SiPM is also named Multi-Pixels Photons Counter (MPPC). The device is chosen because of its low cost and great performance. Hamamatsu's MPPC provides a good PDE with a high fill factor and low voltage required, and by creating a barrier between pixels, they reduced the effect of optical crosstalk.

#### 2.1.2 Instruments

Beyond the resources of the lab, the instruments that I will use are:

- SIGLENT SDS 1104X-E 100 MHz Oscilloscope
- SIGLENT SDS 1202X-E 200 MHz Oscilloscope
- Nice-Power DC Power Supply



(a) SIGLENT Oscilloscope



(b) Nice Power DC Supply

Figure 2.1: Voltage Source and Wave Visualise Instrument

- Readout circuit We made a readout circuit to shape and modify some characteristics of the waveform produced by the MPPC, reduce the noise, and avoid short circuits,... Which we will describe in more detail in the simulation model.



Figure 2.2: MPPC practical readout circuit

- Multi-Pixels Photons Counter (MPPC) Hamamatsu S13360-1325CS



Figure 2.3: Multi-pixels photon counter (MPPC) model S13360-1325CS

Model	S13360-1325CS
Pixel pitch ( $\mu m$ )	$25\mu m$
Number of pixel	2668
Fill factor (%)	47
Operating temperature (degree celsius)	-20 to +60
Spectral response $\lambda$ (nm)	270-900
Terminal capacitance (pF)	60
Gain	$7 \times 10^5$
Breakdown voltage $V_{BR}(V)$	$53 \pm 5$
Recommended operating voltage $V_{OP}$ (V)	$V_{BR} + 5$

Table 2.1: MPPC S13360-1325CS Data sheet [3]

### 2.1.3 Experiment Set-up

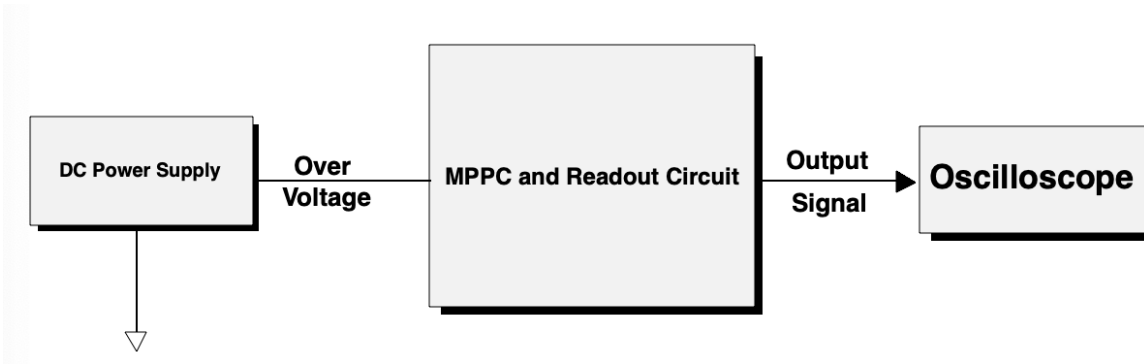


Figure 2.4: Experimental Setup

In the experiment, we coupled the MPPC with the readout circuit. Then we keep the circuit inside the metal box, and this one has the advantage of grounding the circuit, preventing the effect of the electromagnetic wave on the circuit.

For the voltage source, we use the Nice-Power DC Supply. We first increase the voltage until the pulse appears, assuming this is the breakdown voltage. Then to apply the operational voltage, we increase the voltage by  $5V$ .

In the measurement, we conduct the measurement without the effect of the bandwidth

of the amplifier. Thus, the signal's pulse height is very small, in order of a few mV. Therefore, it is essential to reduce electronic noise. The noise was reduced significantly by grounding the circuit well (grounding the box with the instrument's shell). We also need a high resolution Oscilloscope with the bandwidth MHz or above to visualize the signal because the timing resolution is a the scale of ns and a few mV for amplitude, and a high BW limit allows us to have more information about the signal.

## 2.2 Simulation model

### 2.2.1 Assumption

Before doing the simulation, there are a few assumptions that we have to consider:

- The temperature while experimenting is  $25^{\circ}C$
- The performance of the MPPC can be referred to by the datasheet (Gain, Break-down Voltage, Overvoltage, Operation temperature)

### 2.2.2 MPPC and Readout Circuit simulation

This is the circuit we will use in this simulation. The circuit referenced at [5]

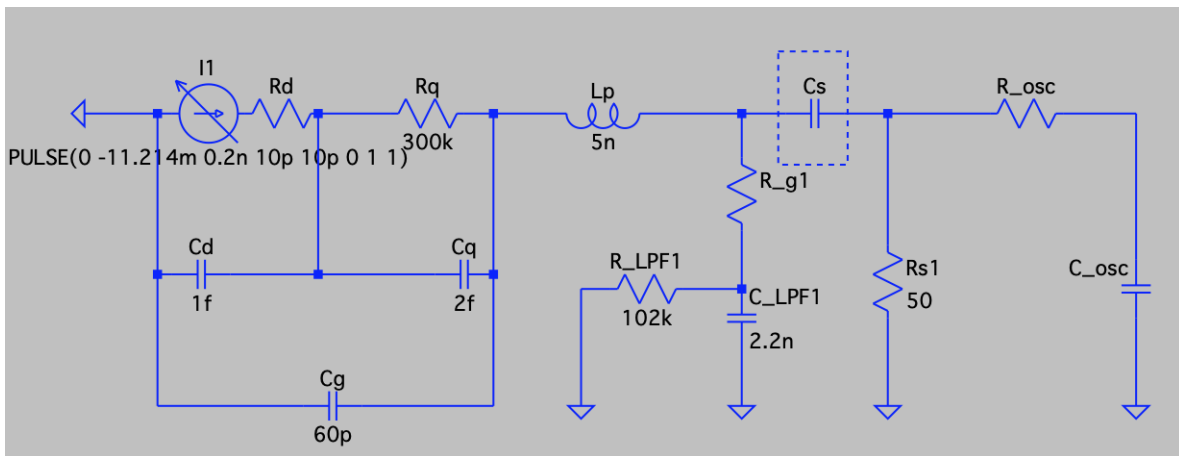


Figure 2.5: Readout circuit for MPPC

The circuit above have four main components:

1. The MPPC equivalent circuit:

- The equivalent circuit for single cell is  $(R_d//C_d)$  in series with  $(R_q//C_q)$ . Where  $R_d$  and  $C_d$  is diode's resistance and capacitance,  $R_q$  and  $C_q$  is the quenching resistance and quenching capacitance,  $C_g$  is the grid capacitance
- The equivalent circuit for the whole MPPC is n pixels in parallel, then all of them in parallel [6].

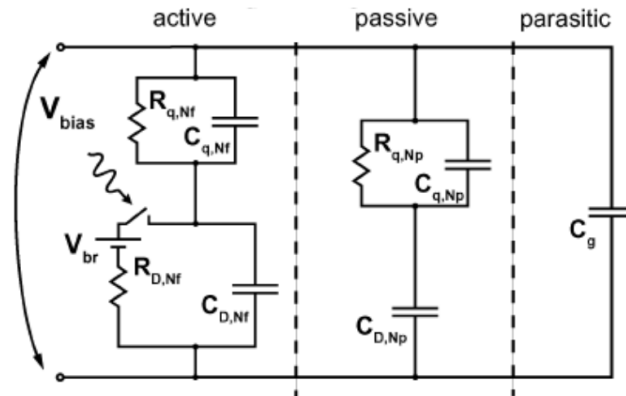


Figure 2.6: Equivalent circuit for the discharged microcells in MPPC [6]

- Our simulation aims to simulate a fired pixel (pixel has signal). We simulated as  $(R_d//C_d)$  in series with  $(R_q//C_q)$ , all of them in parallel with grid capacitor  $C_d$ .
- To simulate the electrical pulse generated by the pixel, we can use the simple estimation:
  - Assumed that the MPPC operates in the normal condition, and the  $V_{bias} - V_{br} = 5V$ . Then from the data sheet of MPPC S13360-1325CS [3], we are expected that is one photon come will produce  $7 \times 10^5$  electrons. Then the total charge will be:

$$1.6 \times 10^{-19} \times 7 \times 10^5 = -11.214 \times 10^{-14} C$$

- Assume an instantaneous burst of avalanche, 10ps of time, then the current of each pulse is

$$I = \frac{Q}{t} = \frac{11.214 \times 10^{-14}}{10 \times 10^{-12}} = 11.214 mA$$

Then the command

PULSE(0 -11.214 0.2n 10p 10p 0 1 1)

Represent for a pulse that rise from 0 to -11.214mA,  $T_{delay}$  is 2ns, then  $T_{rise}$  and  $T_{fall}$  is 10ps.

## 2. Low-pass filter

- the low-pass-filter (LPF) in our circuit represent by a series of resistor (where  $R_{tot} = 102k$  and a capacitor (where  $C = 2.2nF$ )
- The LPF is created to filter out the signal at a high frequency. Where the cutoff frequency is provided by the equation:

$$f_c = \frac{1}{2\pi RC}$$

## 3. Shaping component

- Our shaping component will be  $R_g$  and  $C_s$ . Changing the value of these components will change the shape of our output waveform.
- Due to the scope of this internship report, we will investigate the changing of the shape due to the value of shaping capacitance  $C_s$ . The effect of shaping capacitor to output waveform I will describe in more detail in the waveform signal section.
- Shunt resistor ( $R_s$ ) can avoid the feedback signal and also increase the falling time of the signal

## 4. Bandwidth Limit circuit

- The Bandwidth (BW) limit will be simulated for the Bandwidth limit of the Oscilloscope.
- The BW limit defines the ranges of frequencies that our Oscilloscope can measure more accurately. For small BW, we may not have the correct shape of the signal because some details may be lost. The higher BW provides the higher sensitivity, but if the BW is high enough, we may measure unexpected noise that distorts our signal.

### 2.2.3 Wave form's characteristic

The pulse is composed of two parts: rising and falling.

The ideal model in Figure. 1.3, the pulse shape will have the falling part due to the discharge of the capacitor  $C_d$ , which is  $\tau_{rise} = R_s C_d$ , the falling part due to the recharge of the capacitor (quenching), which is  $\tau_{fall} = C_d R_q$

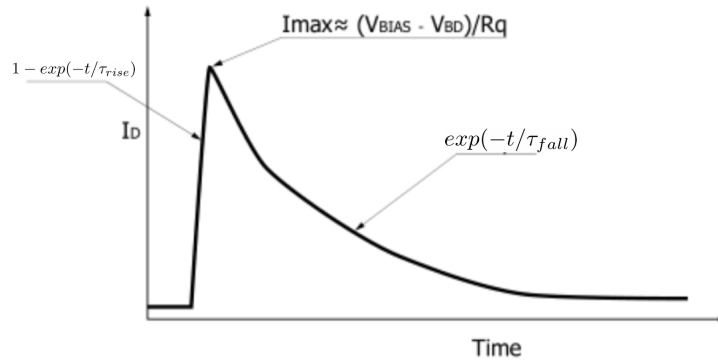


Figure 2.7: Pulse shape for ideal SiPM [1]

For the more practical one, as in Figure. 2.6. The Rising part have the decay time  $\tau_{rise} R_d(C_q + C_d)$ , while the falling part is the sum of two exponential: the first one is the fast decay ( $\tau_{fall,fast} = R_{load}C_{tot}$ ), , the second one is the slow decay ( $\tau_{fall,slow} = R_q(C_q + C_d)$ )

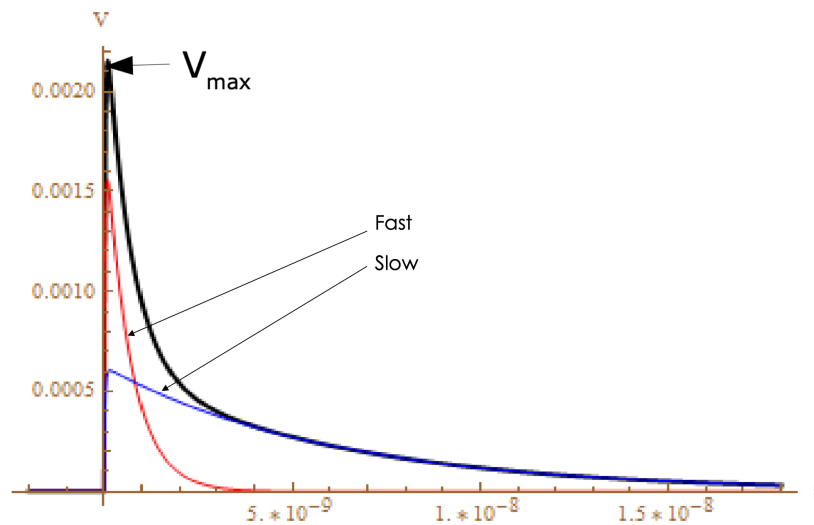


Figure 2.8: Pulse shape in detailed SiPM equivalent circuit [2]

## 2.2.4 Components's parameters

In the circuit of Figure. 2.5. We can obtain some value of MPPC's circuit due to the data sheet.

- The terminated capacitor (or grid capacitor) depends on the sensor size. In the case of MPPC S13360-1325CS, we can obtain the value using the data sheet in table 2.1, which is  $60pF$
- The quenching resistor of a pixel depends on the pixel size; for our model, the pixel pitch is  $25\mu m$ , then the quenching resistance is  $300k\Omega$  [1]
- The shaping capacitor ( $C_s$ ) contribute to the value  $C_{tot}$  in the previous part. Then it affects the decay time, making the pulse sharper.
- From [2], we knew that:

$$G = \frac{\Delta V \times (C_d + C_q)}{q_e}$$

Where  $\Delta V = (V_{bias} - V_{br})$ . In our assumption,  $\Delta V = 5V$ . The Gain  $G = 7 \times 10^5$ . The operation temperature is  $25^\circ C$ . Then

$$C_d + C_q = \frac{G \times q_e}{\Delta V} = \frac{7 \times 10^5 \times 1.602 \times 10^{-19}}{5} = 22.4fF$$

To find out the values of the diode capacitance ( $C_d$ ) and the quenching capacitance ( $C_q$ ), we can make a comparison between the experiment and the simulation and find out the good value for the simulation. First, we need to observe the effect of  $C_d$  and  $C_q$  on the shape of the waveform.

In the figures below, we will show the simulation result of the waveform while changing the value  $C_d$  and  $C_q$ , using the shaping capacitor  $C_s = 0.1\mu F$ , bandwidth  $BW = 200MHz$



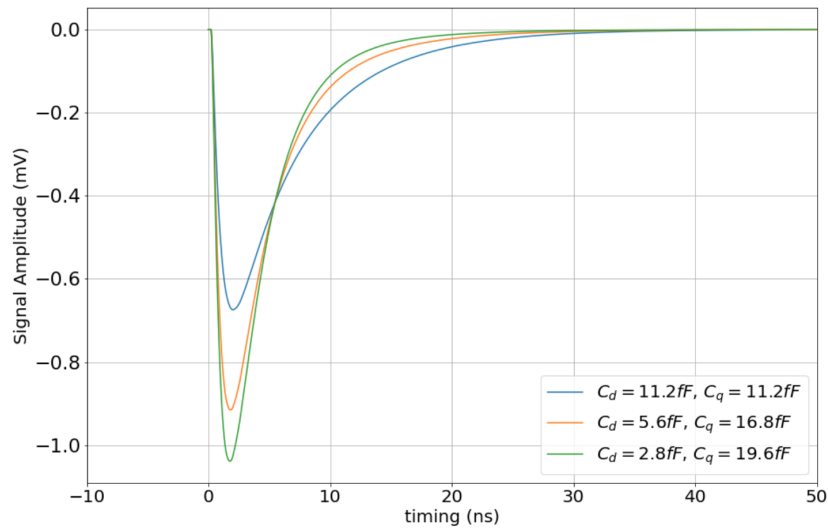


Figure 2.9: Output signal of single P.E waveform simulated by LTspice software when decreasing the value of  $C_d$  and increase the value of  $C_q$ .

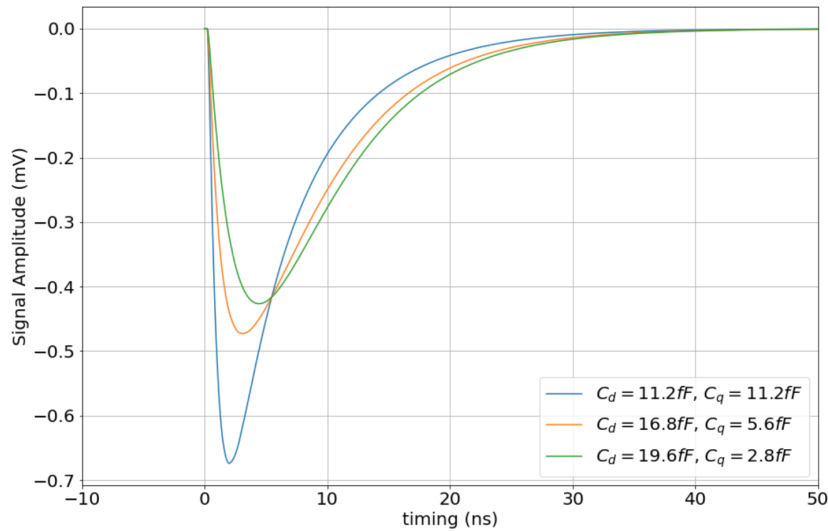


Figure 2.10: Output signal of single P.E waveform simulated by LTspice software when decreasing the value of  $C_q$  and increase the value of  $C_d$ .

From the two figures above, we can see that the two capacitors  $C_d$  and  $C_q$  have the same effect on the waveforms. That is, when the capacitance increase, the amplitude of the waveform increase, and the rising part falling part become steeper. Nevertheless, from figure .2.9, we can easily observe that the amplitude is a dramatic increase when

we increase the value of  $C_d$ , so  $C_d$  has a better effect on increasing the amplitude of the pulse. However, from the figure .2.9, we can figure out that the pulse becomes sharper when decreasing the value of  $C_d$ .

To choose the value that is good for the simulation, we should test the simulation and then try to compare if we can get nearly right the value of  $C_d$ ,  $C_q$  by comparing:

- Pulse shape
- Full-width-half-maximum (FWHM).

In the scope of the simulation, we will choose to value  $C_d = 2.9fF$  and  $C_q = 19.5fF$  because they provide nearly the same shape of the signal peak, and they also provide low error on the value of FWHM.

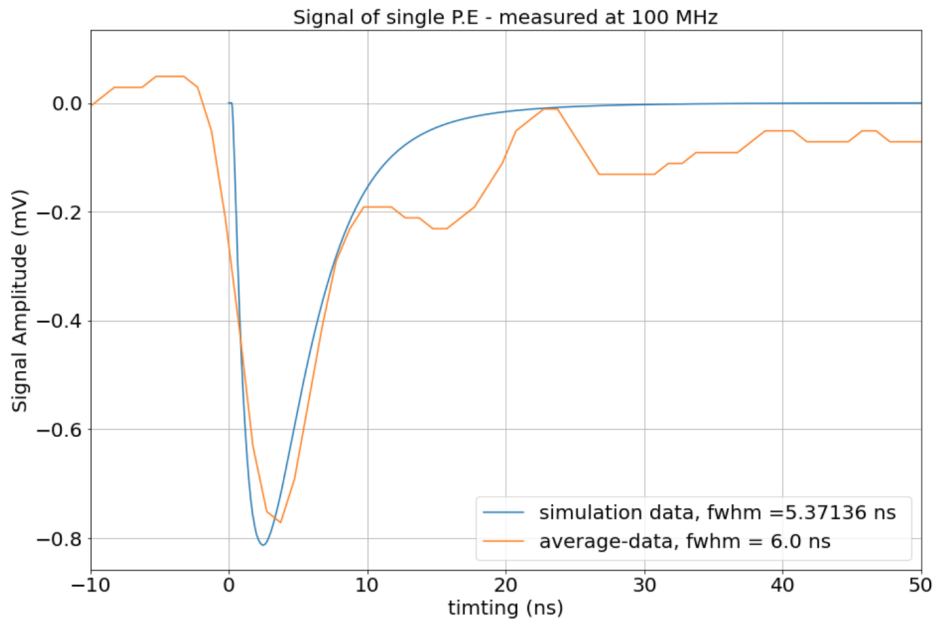


Figure 2.11: The simulation versus the signal measured at BW of 100 MHz. The simulation result simulated by LTspice software, the measurement data is obtained by SIGLENT SDS 1104X-E 100 MHz Oscilloscope.

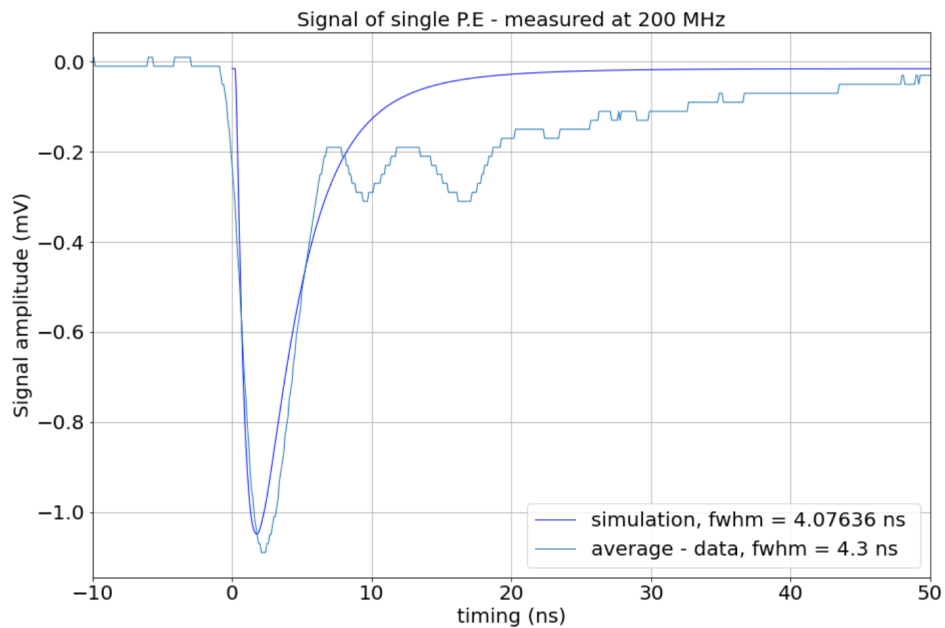


Figure 2.12: The simulation versus the signal measured at BW of 200 MHz. The simulation result simulated by LTspice software, the measurement data is obtained by SIGLENT SDS 1202X-E 200 MHz Oscilloscope.

From the figure. 2.12, we can see that the FWHM of the simulation is closer to the one of the measurement compared to the one in the figure. 2.11. It is because the Oscilloscope we use in the two measurements is different. The Oscilloscope we used in the second experiment has a higher BW limit and provides more data points. Thus, the more data points, the better calculation.

# Chapter 3

## Result and Discussion

### 3.1 Bandwidth Effect to the output waveform

In this part, I will test and observe the effect of BW effect on the output signal. The measurement was conducted using the shaping capacitor with the capacitance  $C_s = 0.1\mu F$  and the one with  $C_s = 1nF$

#### 3.1.1 Simulation result

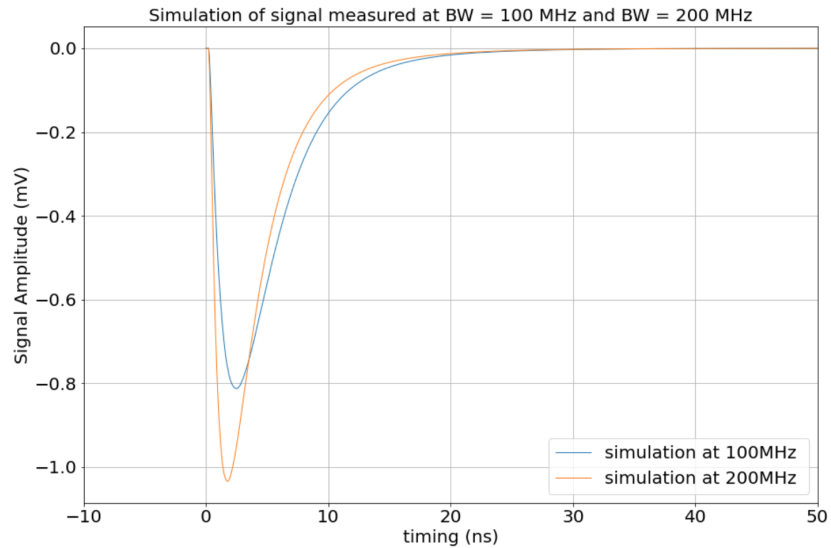


Figure 3.1: Simulated waveforms of the single P.E event generated by LTspice software at different bandwidth limit, using  $C_s = 0.1\mu F$ .

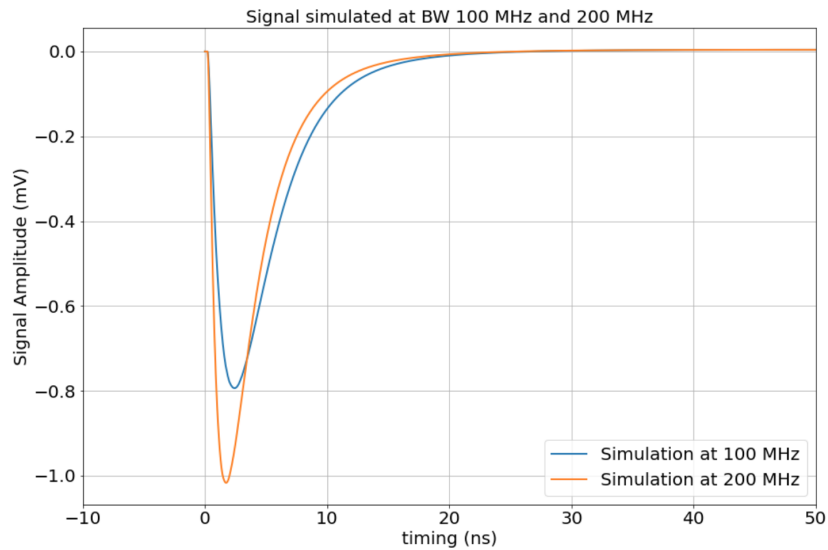


Figure 3.2: Simulated waveforms of the single P.E event generated by LTspice software at different bandwidth limit, using  $C_s = 1nF$ .

In the two above figures, we simulated the pulse of the single P.E event, Performed with two separate circuits with different capacitors. The amplitude of the pulse simulated using shaping capacitor  $C_s = 0.1\mu F$  is slightly higher than that of the shaping capacitor  $C_s = 1nF$ . When comparing the result simulated with different bandwidths, we can observe that the pulse's amplitude became higher with the bandwidth of 200 MHz in both figures. Otherwise, the pulse' shape with the bandwidth of 200 MHz also becomes sharper compared to the bandwidth of 100 MHz.

### 3.1.2 Measurement result

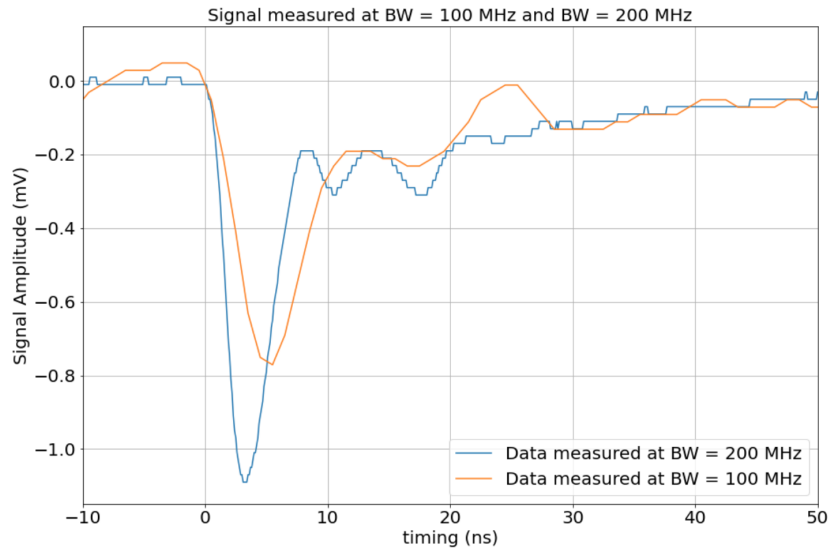


Figure 3.3: Data measured with two different Oscilloscope with different BW limit, using shaping capacitor  $C_s = 1\mu F$ . Both pulses is averaged with 256 samples.

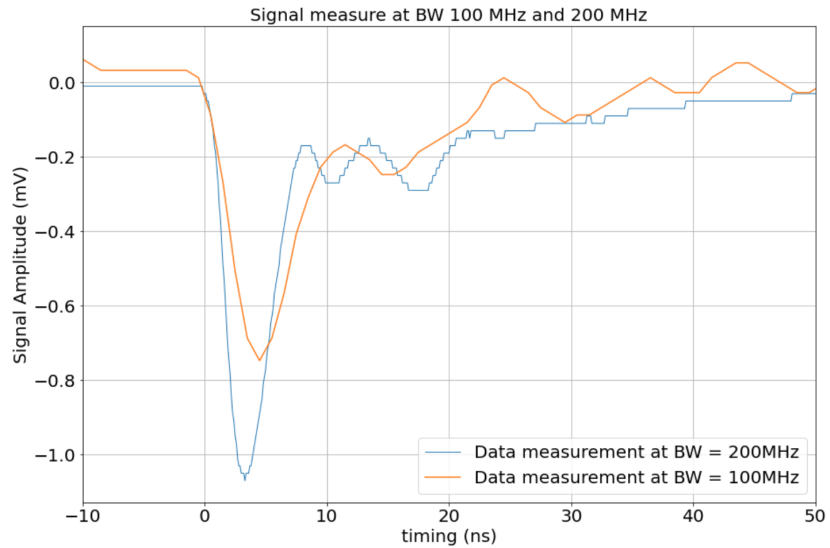


Figure 3.4: Data measured with two different Oscilloscope with different BW limit, using shaping capacitor  $C_s = 1nF$ . Both pulses is averaged with 256 samples.

In the measurement result, the signal is the combination of the primary signal, dark noise, and the after-pulse, which is reasonable to the oscillate in the tail (the falling

period) of the pulse. The pulse also oscillates before the rising period, so we did an average and then offsetting to the neutral line ( $y = 0$ ). The little difference in behavior is based on data taken from two oscilloscopes. As expected from figure 3.1 and figure 3.2, we can observe the higher amplitude and the sharper pulse with 200 MHz BW data as expected from the simulation result.

## 3.2 Effect on waveform due to shaping capacitor

In this section, we will show the resulting waveform collected when changing the value of the shaping capacitor ( $C_s$ ). For the test, we will use five capacitors with capacitance  $C_s = 47pF, 220pF, 1nF, 10nF, 0.1\mu F$ , in two different bandwidth (100 MHz and 200 MHz)

### 3.2.1 Simulation result

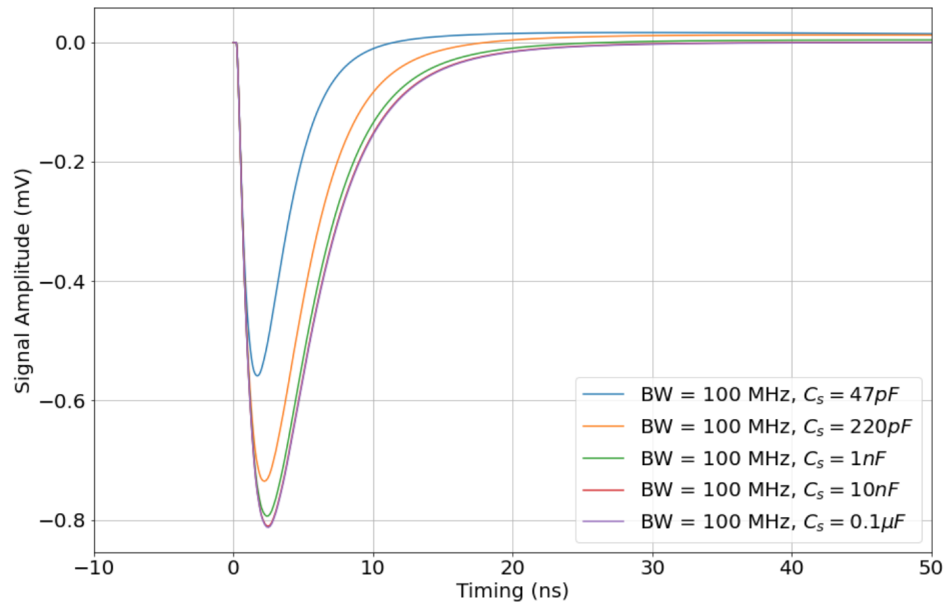


Figure 3.5: Simulation results of output waveforms using different capacitors, at BW = 100 MHz.

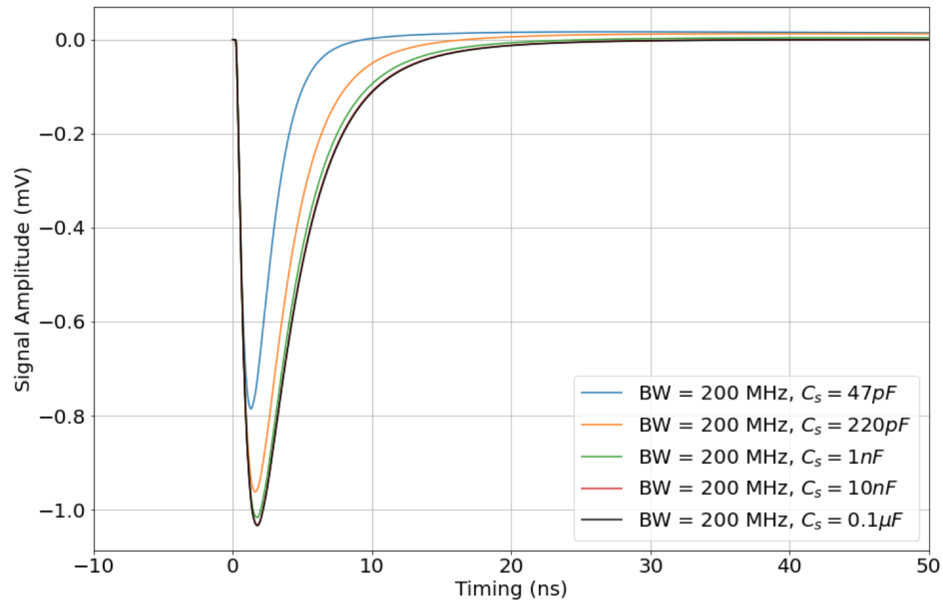


Figure 3.6: Simulation result of output waveforms using different capacitors, at BW = 200 MHz.

The simulation pulse above is simulated the pulse of the single P.E event, with two different circuits as figure. 3.1 and the figure. 3.2. From the two figures, we can recognize the increasing in amplitude when increasing the capacitance (from  $47\text{pF}$  to  $0.1\mu\text{F}$ ). However, the signal's pulse width also increase with the shaping capacitance. In the pulse generated by the circuit with  $C_s = 47\text{pF}$ , we can realise that the signal's amplitude caused an overshoot when exceed the neutral line ( $y=0$ ).



### 3.2.2 Measurement result

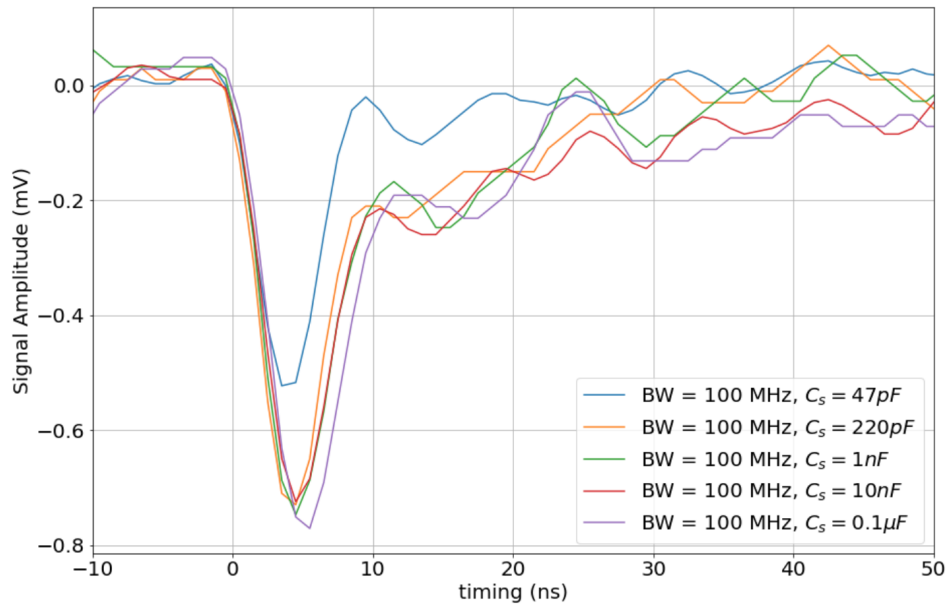


Figure 3.7: Experimental results of the single P.E output waveforms, measured with different capacitors, the data is obtained using SDS 1104X-E 100MHz Oscilloscope.

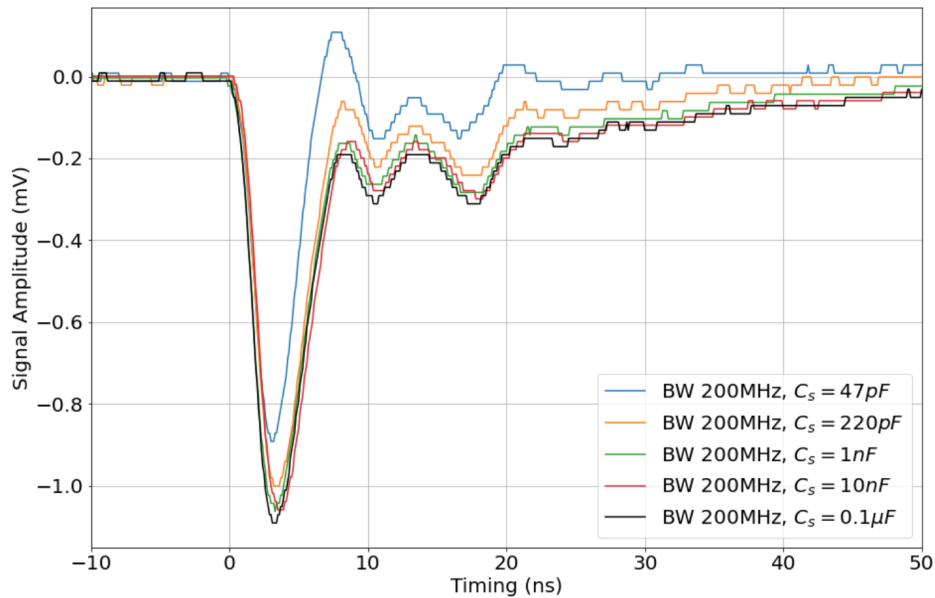


Figure 3.8: Experimental results of the single P.E output waveforms, measured with different capacitors, the data is obtained using SDS 1202X-E 200MHz Oscilloscope.

From both figures above, we can observe the result as expected. 3.5 and figure. 3.6. That is, the pulse width becomes sharper using a low capacitance value. When measuring at high value ( $C_s = 1nF, 10nF, 0.1\mu F$ ), the amplitude does not change so much. There is another result: we can observe the overshoot clearer at  $BW = 200$  MHz; using this BW, we can see more detail about the signal. Despite the overshoot effect, an improvement in the decay time was also observed. It is possible to reduce the overshoot effect by combing some additional electronic devices into the circuit. After that, the timing resolution of MPPC can be improved by changing the shaping capacitor. The behavior we observed is from the signal of a single P.E event; it would be fascinating to explore with a larger signal (from a few tens to a few hundred P.E) since this is the signal range typically used.

# Chapter 4

## Conclusion

During a two-month internship, I had a chance to study not only the MPPC's properties but also electronic circuit simulation with advanced sensors and the effect of bandwidth and the shaping capacitor on the output waveforms. The internship at Neutrino lab also allows me to have some hands-on experiments and enrich my skills handling those equipment.

However, there is some work that I have not done yet. I wish to explore more about the experiment by testing a broader range of shaping capacitance values and having the precise value for the diode capacitance and quenching capacitance. Knowing these things and having good measurement results, we can apply those to study more profound about the MPPC and its applications.

# Chapter 5

## Appendix

### 5.1 Obtain the mean life time of the pulse using exponential fitting

The Signal pulse generated by the MPPC has the form of two half exponential functions. We can obtain how fast the signal discharge by observing the measurement data. To define this rate, we have a general equation:

$$y = e^{-\lambda x}$$

Where  $\lambda$  is the decay rate, a dimensionless parameter. For the negative exponential  $e^{-\lambda x}$  (decay), the higher the value of  $\lambda$ , the faster the exponential decay.

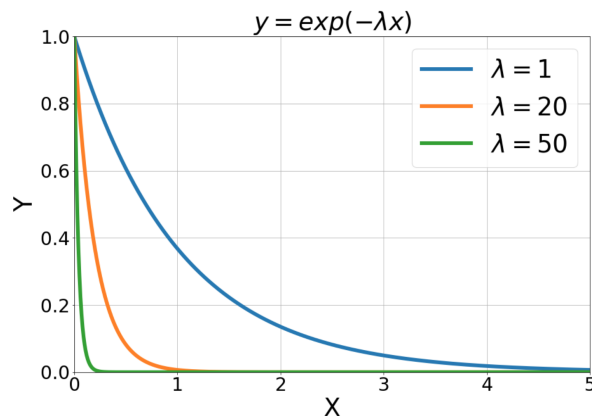


Figure 5.1: Exponential decay

Opposite to that, we have "mean lifetime", where  $\tau = \frac{1}{\lambda}$ , which has the same di-

mension as the horizontal axis. In the pulse shape, we will divide the fitting region into two main parts: the rising and falling times. Where:

- Rising time: the time it takes for the pulse to increase from 10% to 90% maximum.
- Falling time: the time it takes for the pulse to decrease from 90% to 10% maximum.

In the report's scope, I will show the result of fitting data in the rising part because the falling part is highly affected by the after-pulse. For the data, I use the data of a 200 MHz Oscilloscope; since this one has higher resolution, we have more data points for the same period. Thus, the better result (another reason is that the number of data points provided by 100 MHz Oscilloscope in our fitting region is very small, leading to a bad fitting result). Then to check if the fitting is good or not, I use the chi-square equation:

$$\chi^2 = \sum_{i=1}^n \frac{(x_{obs} - x_{exp})^2}{x_{exp}}$$

Where  $x_{obs}$  is the observable data from the experiment,  $x_{exp}$  is the expected value obtained from the fitting. From the equation, we realize that the smaller  $\chi^2$ , the better the fitting result.

The fitting region will have the exponential form; then I will define the general equation that we will use to fit:

$$y = a - c \times (e^{-bt})$$

Where  $a$  is the offset parameter on the vertical axis,  $c$  is the amplitude parameter,  $b$  is the decay rate. We can get the value "mean lifetime" by inverting the value of  $b$

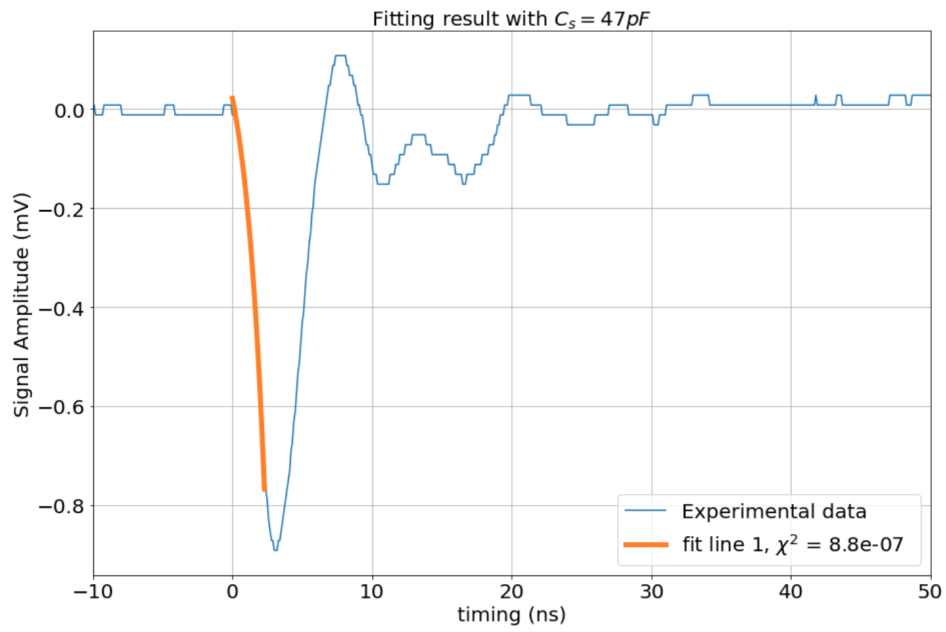


Figure 5.2: Result of shaping capacitor  $C_s = 47pF$

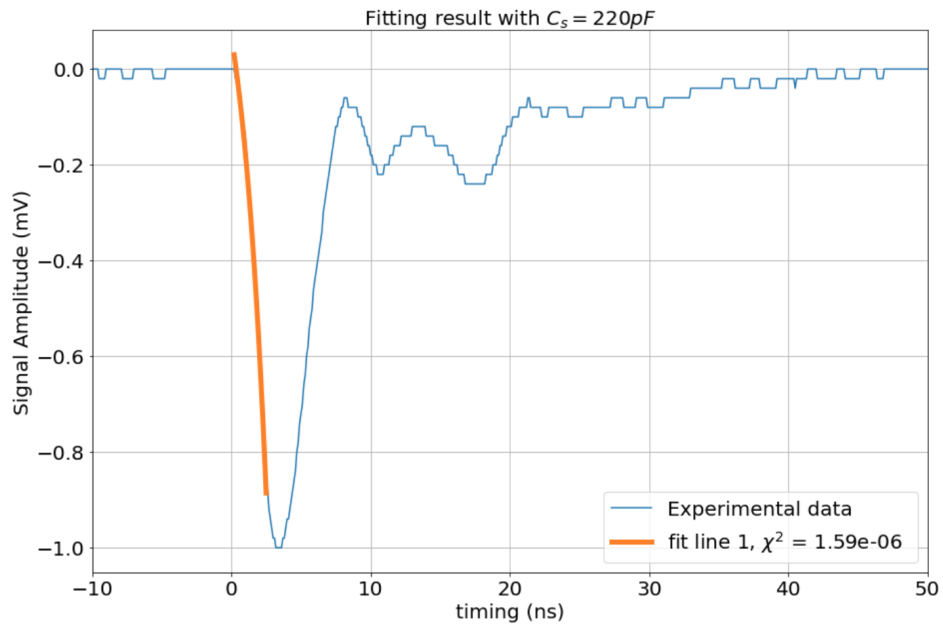


Figure 5.3: Result of shaping capacitor  $C_s = 220pF$

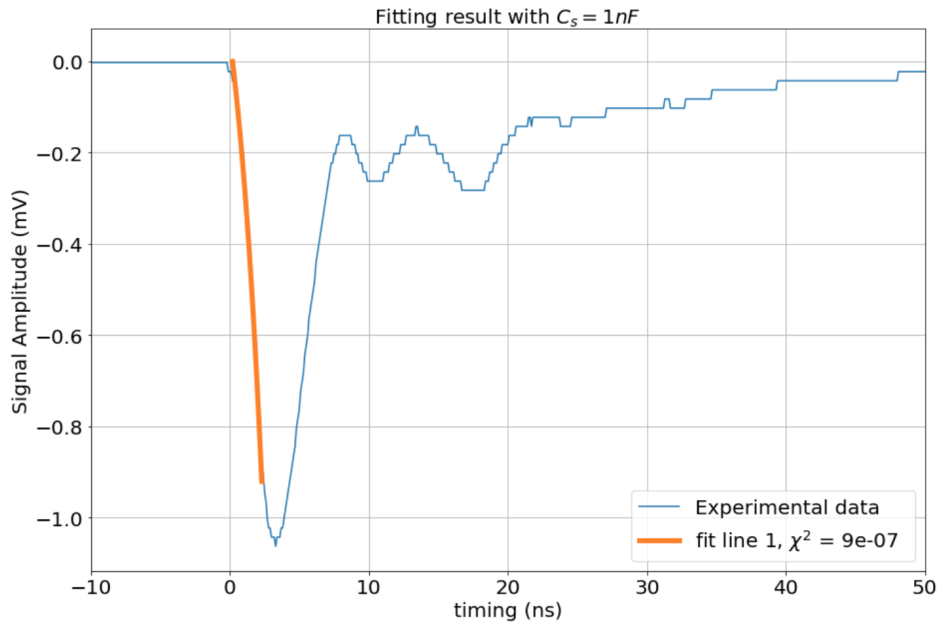


Figure 5.4: Result of shaping capacitor  $C_s = 1nF$

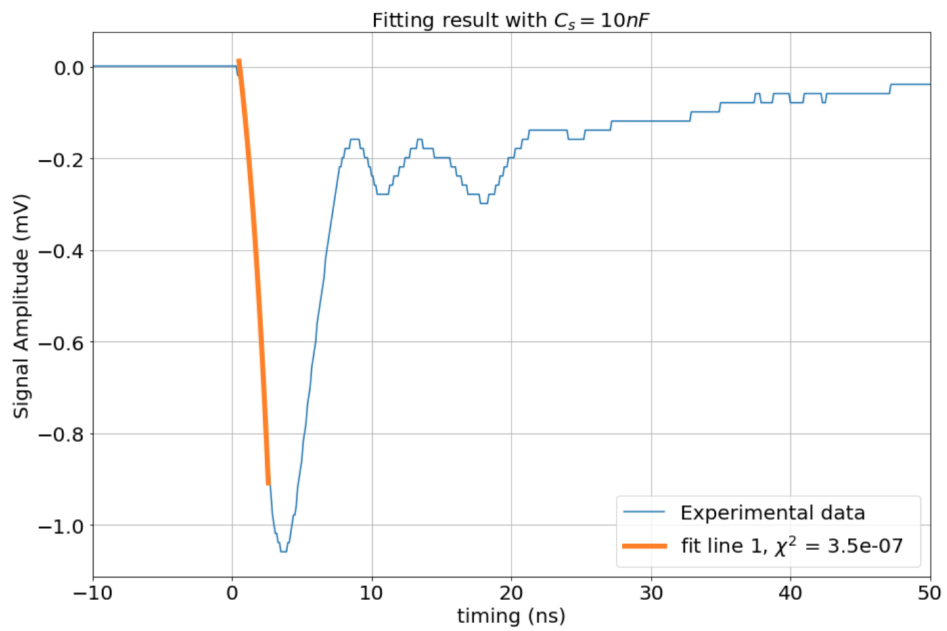
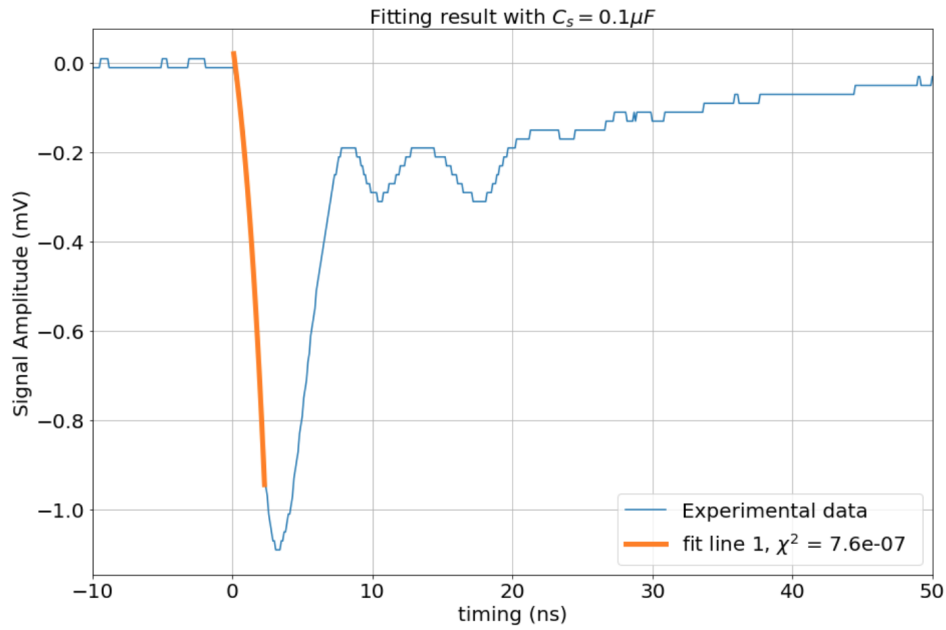


Figure 5.5: Result of shaping capacitor  $C_s = 10nF$


 Figure 5.6: Result of shaping capacitor  $C_s = 0.1\mu F$ 

Capacitance	Rising Time (ns)	Mean lifetime	$\chi^2$
$47pF$	2.3	1.44507	$8.8e-7$
$220pF$	2.3	1.90102	$1.59e-6$
$1nF$	2.1	2.14319	$9e-7$
$10nF$	2.1	2.08872	$3.5e-7$
$0.1\mu F$	2.2	1.93617	$7.6e-7$

Table 5.1: Parameter obtained from the fitting

From the result at table 5.1, we can observe that at the range  $1nF, 10nF, 0.1\mu F$ , the mean lifetime does not change so much. But it decreased significantly when decreasing the capacitance of the shaping capacitor.



# Bibliography

- [1] K. Kobayashi A. Ghassemi, K.Sato. Mppc literature. MPPC, 2021.
- [2] G.Collazuol. The sipm physics and technology, 2012.
- [3] Hamamatsu. Mppc s13360 series.
- [4] Hamamatsu. Mppc technical note.
- [5] N. H. Duy Thanh, and others. Multi-pixel photon counter for operating the tabletop cosmic-ray detector under loosely controlled conditions. 2021.
- [6] Stefan Seifert, and Herman T. van Dam. Simulation of silicon photomultiplier signals. IEEE Transactions on Nuclear Science 56(6), January 2010.